Characterization of Extractable Metals from the Aquifers with Arsenic Contamination in the Tsengwen Creek, Taiwan

Hsueh-Yu LU

Department of Earth and Environmental Sciences, National Chung Cheng University,
Min-Hsiung Chia-Yi, Taiwan

Abstract

Lu H.-Y. (2014): **Characterization of extractable metals from the aquifers with arsenic contamination in the Tsengwen Creek, Taiwan**. Soil & Water Res., **9**: 66–76.

Arsenic contamination in groundwater is a common groundwater problem worldwide. To manage groundwater resources effectively, it is crucial to determine the arsenic source. Taiwan's Tsengwen Creek watershed is one of the known areas for groundwater arsenic contamination. Water-rock interactions are evaluated on a regional scale. A conceptual hydrogeological framework is first established based on groundwater hydrochemistry. The local aquifer system can be categorized into high-arsenic deep aquifer and low-arsenic shallow aquifer. The average geochemistry of sediments indicates that arsenic and heavy metals are not significantly enriched in the deeper aquifer on the scale of the whole watershed. Therefore, arsenic contamination in the deeper groundwater of the Tsengwen Creek watershed is not simply source-controlled. However, the Fe-Mn oxides in sediments contain slightly more arsenic in the deep aquifer. The long residence time of groundwater could magnify the enrichment and cause natural arsenic contamination in the deep aquifer.

Keywords: BCR sequential extraction procedure; groundwater hydrochemistry; sediment geochemistry

Arsenic is a highly toxic metalloid. Arsenic ingestion not only increases the risk of developing cancer of the skin, internal organs, and lungs but also causes a peripheral vascular gangrene disease known as black-foot disease (Tseng *et al.* 1961; Lu 1990). Arsenic contamination of groundwater and its health impact on people has been reported worldwide. Additionally, given that approximately 70% of the world's population lives in coastal areas, the demand for agricultural, industrial, and domestic water use is much higher there than in inland areas and more sources of contamination are present due to increased human activities. Under such conditions, groundwater resource management has become more critical in balancing the extreme non-uniform rainfall distribution in both spatial and temporal domains.

In this study, the Tsengwen Creek watershed is examined because it is known for high arsenic content problems in groundwater (e.g. Tseng *et al.* 1961; Lu 1990; Li *et al.* 2011). Extensive efforts have been made to understand the geochemical transformation of arsenic in the groundwater of the Chianan Plain (e.g. Liu *et al.* 2003; Wang *et al.* 2007; Selim Reza *et al.* 2012). These studies demonstrate very important results based on groundwater hydrochemistry and sediment geochemistry. In general, the low redox state and high content of humic substance were suggested to be the mechanism for arsenic contamination in groundwater. However, the aquifer system of the Tsengwen Creek watershed is characterized by relatively low hydraulic conductivity values (Lu *et al.* 2008). Under these circumstances, it is crucial to evaluate water-rock interactions on a regional scale. In this study, the sediment geochemistry and groundwater hydrochemistry were examined with statistical analyses on the basis of aquifer average and individual samples.

MATERIAL AND METHODS

Regional geology. The Tsengwen Creek is located in southwestern Taiwan and ranks as the fourth long-

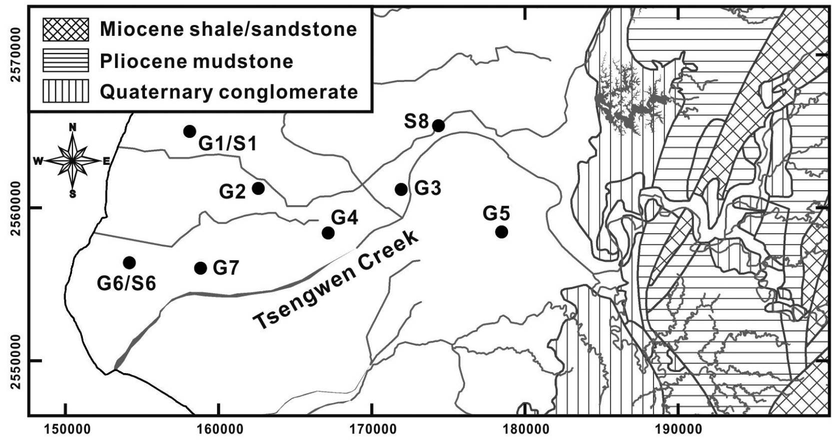

Figure 1. Topographical map of the Tsengwen Creek watershed showing the sampled localities
G – groundwater, S – sediment

est and largest river. The river starts in the mountain areas of Central Taiwan (Figure 1). It drains an area of about 1177 km^2. Sedimentological studies have reconstructed the geographical evolution of the Tsengwen Creek alluvial plain (Hsieh & Knuepfer 2001). During the last glacial period (> 15 000 years ago), most of the study area was exposed (Figure 2a). The aquifers deposited in this period range from 120 to 250 m in depth and have relatively higher conductance. After the last glacial maximum, most of the Tsengwen alluvial plain was inundated after the global sea-level change as shown in Figure 2b. An extensive aquitard was deposited above the glacial aquifer system during the post-glacial period. This sea-level transgression ended about 7000 years ago but the coastal plain still experienced a lagoon to estuarine environment for thousands of years (Figure 2c). This depositional environment subsequently resulted in a shallow aquifer system with a relatively poor conductance. As shown in Figure 2d, until the 18th century, the historic record shows the coastal line retreating at a high rate toward the Taiwan Strait. The Tsengwen alluvial plain is now again exposed to above sea level.

Sampling and pre-treatment of samples. Two kinds of samples were collected: groundwater and aquifer sediments. Groundwater samples were collected from 7 sites around the watershed of the Tsengwen Creek (Figure 1) during July 2010. The samples and their depths are listed in Table 1. Prior to collecting water samples, at least three well casing volumes of water were purged. After purged, the groundwater was extracted and immediately filtered through a 0.45 μm glass fibre paper. For cation analysis, the samples were acidized to pH < 2 with ultrapure nitric acid. The samples for anion analysis were stored at 4°C and shipped to the laboratory within 12 h.

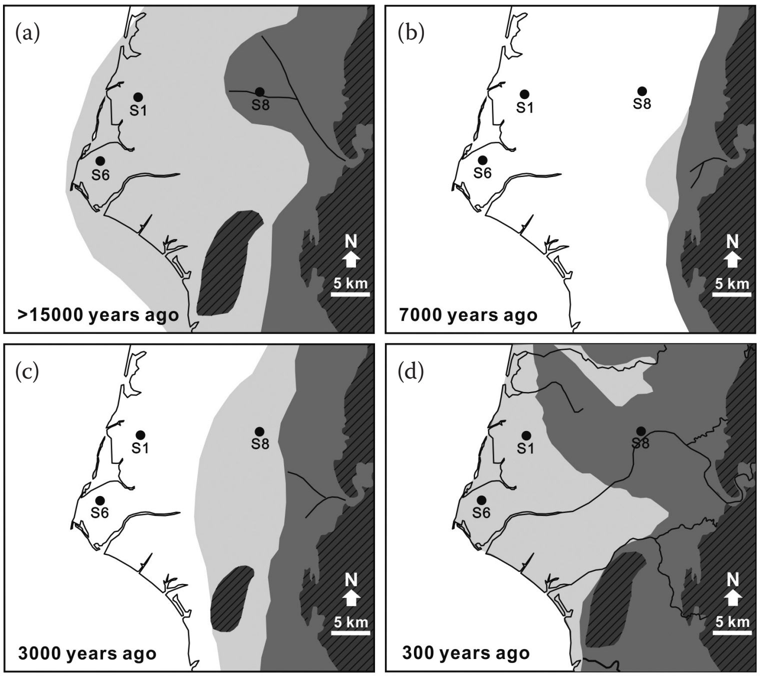

Figure 2. Geographical evolution of the Tsengwen Creek alluvial fan: (a) > 15 ka, (b) 7 ka, (c) 3 ka, and (d) 0.3 ka; the solid circle denotes locations of sediment samples (Hsieh & Knuepfer 2001)

Table 1. General hydrochemical properties and major constituents of groundwater in the Tsengwen Creek watershed

Sample	Depth* (m)	pH	EC (µS/cm)	ORP (mV)	HCO_3	F	Cl	Br	NO_3	SO_4	Na	Mg	K	C)	Mn	Fe	Sr
											(ppm)						
G1-1	37	8.75	> 20 000	–376	234.9	nd	29 347.2	23.3	nd	5 759.9	33 459	2 587	854	544	2.23	nd	9.03
G1-2	235	7.42	1 115	–253	292.8	0.09	118.7	0.6	0.7	9.3	526	10	4	21	0.03	0.19	0.22
G2-1	39	Na	na	na	210.5	na	na	na	na	na	13 070	661	290	352	0.45	nd	7.78
G2-2	111	Na	na	na	347.7	na	na	na	na	na	16 353	717	311	349	nd	1.47	10.23
G2-3	140	6.84	11 930	–163	280.6	nd	7 422.3	5.3	0.4	6.5	6 668	309	116	172	0.09	nd	4.18
G2-4	236	7.49	657	–189	427.0	0.14	121.4	0.4	nd	nd	289	6	5	8	0.06	0.31	0.14
G3-1	48	6.84	967	–121	210.5	0.16	7.6	nd	nd	nd	26	40	5	126	0.17	0.09	0.84
G3-2	214	6.79	552	–131	268.4	0.19	370.1	0.3	nd	0.1	246	34	3	84	0.08	0.01	0.71
G4-1	32	7.09	1 917	–286	30.5	0.72	360.7	0.2	nd	7.7	339	32	34	52	0.13	0.01	0.36
G4-2	69	6.63	> 20 000	–277	533.8	1.78	18 769.3	13.3	9.5	2 199.2	2 453	157	48	62	1.99	nd	11.99
G4-3	245	7.19	1 084	–260	384.3	0.26	36.6	0.3	0.3	2.2	204	11	4	26	0.19	0.01	0.25
G4-4	289	7.10	1 853	–326	152.5	0.32	210.5	0.1	nd	11.6	381	28	7	39	0.01	nd	0.02
G5-1	38	6.86	678	–122	338.6	na	na	na	na	na	27	20	4	80	0.12	0.46	0.46
G5-2	102	6.79	552	–131	341.6	na	nd	na	na	na	105	19	4	70	0.05	1.63	0.37
G6-1	34	7.05	> 20 000	–206	161.7	0.19	22 063.0	19.6	0.5	4 271.0	22 129	1 604	516	505	1.05	nd	10.08
G6-2	209	7.47	16 510	–371	646.6	0.18	4 357.0	0.6	0.3	474.9	6 491	372	148	120	nd	nd	2.32
G6-3	278	8.45	2 460	–66	713.7	0.59	267.1	0.2	nd	0.4	694	2	14	1	0.03	0.62	0.05
G7-1	69	7.03	> 20 000	–417	439.2	nd	22 532.9	14.1	nd	1 942.3	26 267	1 721	559	384	nd	nd	11.17
G7-2	230	6.68	8 010	–267	237.9	nd	1 737.4	1.1	nd	nd	776	95	15	149	0.12	4.83	1.74

*in meters below the sea level; nd – concentration cannot be detected with inductively coupled plasma mass spectrometry; na – concentration is not analyzed; EC – electrical conductivity; ORP – oxidation reduction poptential

The aquifer sediments were sampled from 3 sites along the groundwater flow path from the east to the west coast (Figure 1). A total number of 49 sediment samples were taken only within the aquifers being monitored. Each sample was obtained by cutting rock core samples of 5 × 1 cm. In the laboratory, the thin skin of all samples was carefully removed with a ceramic knife. The original samples were then dried in an oven at 105°C for 3 h and were mildly grounded with an agate mortar so as to pass through a 200-mesh sieve.

BCR SEP. X-ray diffraction analysis (XRD) is the most popular method to identify mineralogical assemblage of soils. However, it is difficult to obtain quantitative results if the amounts of minerals were minor. Alternatively, BCR SEP was designed with a three-step extraction procedure to determine the extractable trace metals in soil and sediment (e.g. Ure *et al.* 1992; Whalley & Grant 1994). This method is also applicable to quantitatively determine the extractable arsenic in soils (e.g. Baig *et al.* 2009). The BCR SEP procedure aims to fractionate metals into the operationally defined components of acid extractable (exchangeable and carbonates), reducible, oxidizable, and residuals in soil. In this study, an improved BCR 3-step procedure was followed as per Rauret *et al.* (1999). The extraction procedure starts with 1 g of pre-treated original material. During the first step, metals from exchangeable and carbonate phases were extracted with 40 ml of 0.11 mol/l acetic acid at room temperature for 16 h. Step 2 used reagent solution of 0.5 mol/l $NH_2OH{\cdot}HCl$, which was adjusted to pH = 2 with nitric acid. The samples were extracted with 40 ml of this reagent at room temperature for 16 h. In step 3, 30% H_2O_2 adjusted to pH = 2–3 with nitric acid was used to break down organic matter. The residue was subsequently extracted with 50 ml of 1.0 mol/l NH_4OAc (pH = 2.0) for 16 h. The residue of the three-step sequential extraction represents mineral phases that are hard to be released; therefore, the final step of BCR SEP, was not conducted in this study.

Chemical and statistical analyses. In the field, groundwater properties were measured using Horiba D-54 for temperature, pH, electrical conductivity (EC), and oxidation reduction potential (ORP). In the laboratory, the original water samples were used to determine anions by a Dionex ICS-90 (Dionex, Sunnyvale, USA) whereas cation analysis was conducted on acidized water samples with Perkin Elmer ICP-OES 4300DV (Perkin Elmer, Waltham, USA) (ppm level) and Agilent 7500cx ICP-MS (Agilent, Santa Clara, USA) (ppb and ppt levels). The precision was determined with the standard deviation of three individual runs, and must be better than 10%. The accuracy was evaluated by repeated measuring the extracted solution of the certified reference sediment CRM601 (IRMM, Geel, Belgium) in every 10 sample measurements. The unqualified results in between two repeated measurements would be discarded.

Multivariate statistical analysis of water chemistry has been successfully applied to elucidate hydrological processes and hydrochemical evolution (e.g. Anazawa & Ohmori 2005; Irawan *et al.* 2009). In this study, cluster analysis (CA) was utilized to categorize the hydrochemistry of groundwater in the Tsengwen Creek watershed for the first-order approach. In addition, R-mode factor analysis (FA) is a technique used for reducing variables (measured geochemical constituents in this study) to a smaller number of new factors. The new factors can be interpreted by geochemical processes according to the similarity among highly correlated variables (e.g. Farnham *et al.* 2003; Bošnjak *et al.* 2012). There are several factor extraction methods – in this study, the factors were extracted with Principal Components Analysis and Varimax normalized rotation was applied to achieve higher loadings of variables.

RESULTS AND DISCUSSION

General groundwater hydrochemistry. In general, groundwater in the study area shows near neutral to alkaline pH (6.68–8.75) and highly reduced redox condition ranging between –417 to –66 mV as shown in Table 1. These properties are common among most of the groundwater samples. However, the groundwater of the Tsengwen Creek watershed is prominently characterized by high salinity, especially in the shallow groundwater. The Na concentrations of G2-1 and G7-1 are all over 15 000 ppm (Table 1) and both sites are located at about 8 km inland (Figure 1). This is mostly caused by the presence of low hydraulic conductivity, which resulted in entrapped paleo-brackish waters. Seawater intrusion is not a likely cause of saline water because the high-salinity groundwater frequently occurred in unreachable inland areas as mentioned. This is also confirmed by the regional geology that most area of the watershed had still been submerged under the sea until 300 years ago (Hsieh & Knuepfer 2001).

CA on groundwater hydrochemistry. To establish a hydrogeological framework based on hydrochemical data, CA is an excellent tool for dividing data into groups that have distinct chemical properties (e.g.

Table 2. Minor and trace metals in groundwater of the Tsengwen Creek watershed

Sample	Li	V	Ni	Cu	Zn	As	Se	Ba	Cr	Co	Cd	Pb	U
					(ppb)						(ppt)		
G1-1	2.2	1.5	0.6	330.4	nd	28.0	19.1	55.1	nd	91	nd	5	nd
G1-2	5.8	1.6	4.8	2.5	10.9	927.3	1.2	64.2	365	467	nd	67	3
G2-1	5.7	5.3	1.4	148.4	2.2	16.4	44.1	108.7	nd	392	nd	43	20
G2-2	2.6	3.9	0.9	183.3	nd	58.3	37.3	7771.0	nd	211	nd	20	nd
G2-3	5.7	4.4	8.5	65.7	8.0	88.0	40.7	2538.0	102	600	nd	12	8
G2-4	4.3	1.6	0.6	3.2	3.8	669.6	1.6	54.5	185	305	6	79	3
G3-1	3.7	0.3	1.8	nd	12.9	54.7	0.8	107.0	nd	232	nd	10	30
G3-2	6.8	0.9	1.2	0.7	340.2	477.9	3.6	158.4	43	403	nd	55	nd
G4-1	10.7	1.2	1.4	1.1	2.2	70.1	3.5	104.1	143	155	nd	1254	3
G4-2	2.7	2.4	1.5	287.4	3.9	4.3	25.0	166.1	nd	352	nd	nd	22
G4-2	6.8	0.8	1.2	1.2	nd	362.3	0.7	58.6	72	199	5	47	5
G4-4	7.4	1.0	5.5	1.3	29.6	334.9	2.6	176.6	478	419	nd	60	4
G5-1	3.7	0.7	1.1	nd	nd	54.2	0.8	142.7	nd	123	nd	121	10
G5-2	6.4	0.9	0.8	nd	nd	526.0	0.9	96.8	14	183	nd	6	nd
G6-1	3.7	2.0	0.6	210.9	0.4	6.7	26.2	51.8	nd	144	nd	4	30
G6-2	4.5	6.2	1.5	53.5	1.8	312.9	31.0	68.5	358	482	nd	31	3
G6-3	3.7	12.4	1.5	5.4	nd	143.2	2.8	13.2	296	523	nd	492	12
G7-1	3.4	2.0	0.4	209.9	nd	5.4	23.7	46.5	68	100	nd	nd	4
G7-2	10.1	1.2	3.2	8.8	9.8	452.0	13.1	734.3	91	454	nd	108	nd

nd – concentration cannot be detected with inductively coupled plasma mass spectrometry

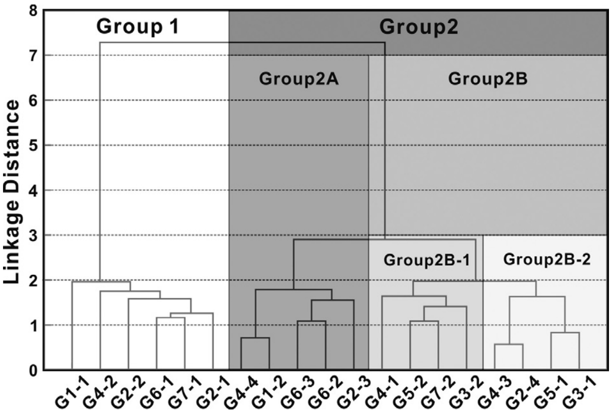

Figure 3. Dendrogram from the cluster analysis (CA), which is based on rescaled hydrochemical values in the Tsengwen Creek

Guggenmos *et al.* 2011). A hierarchical clustering algorithm was performed and the distances between groups were calculated with Ward's method. The dendrogram from the CA separates the samples into two groups based on EC in the first-order approximation (Figure 3). All groundwater of Group 1, including G1-1, G2-1, G2-2, G4-2, G6-1, and G7-1, was sampled in the mid- to downstream area from depths shallower than 120 m. These samples share the hydrochemical property of very high EC levels, which is representative of infiltration from evaporated seawater due to the lagoon environment 15 000 years ago in this area (Hsieh & Knuepfer 2001). By contrast, the groundwater of Group 2 has relatively low EC values. In this group, a subgroup of Group 2A can be identified with deep samples (> 200 m) in the mid- to downstream area, which possibly promoted the effect of cation exchange between Ca^{2+} and Na-Clay. The other group (Group 2B) shows no considerable cation exchange but shares the lower EC levels. CA can further be used to divide Group 2B into Group 2B-1 and Group 2B-2 whereby Group 2B-1 is characterized by the hydrochemistry of deep groundwater in the upstream area (G3-2 and G5-2) and Group 2B-2 by the hydrochemistry of shallower groundwater in the upstream area (G3-1 and G5-1). However, both subgroups contain very deep groundwater (> 200 m) in the mid- to downstream areas (G2-4, G4-3, and G7-2). This implies that some samples taken at depth in the downstream area may have experienced only limited seawater infiltration, which is similar to samples taken further upstream. Sample G4-1 in Group 2B-1 is expected to appear in Group 1 with very high EC such as G4-2, the deeper sample in the same site (Figure 3). It is believed that the low EC of G4-1 results from dilution by modern freshwater. However, this is just one of the possibilities. More evidences would be needed to confirm the derivation.

Conceptual hydrogeological profile and arsenic spatial distribution. According to the above discussion of regional hydrogeology and CA, a conceptual hydrogeological profile can be established as shown in Figure 4, which demonstrates a two-layer aquifer system. The system includes two aquifers separated by an extensive aquitard deposited during the postglacial transgression period. A very high level of Na concentration can be observed in the shallow aquifer due to lagoon environment while the deep aquifer has lower salinity (Figure 4). Figure 4 also shows the arsenic spatial distribution along the hydrogeological profile. All groundwater from the deep aquifer contains arsenic of > 100 ppb. For the shallow groundwater, the arsenic content generally decreases from up- to

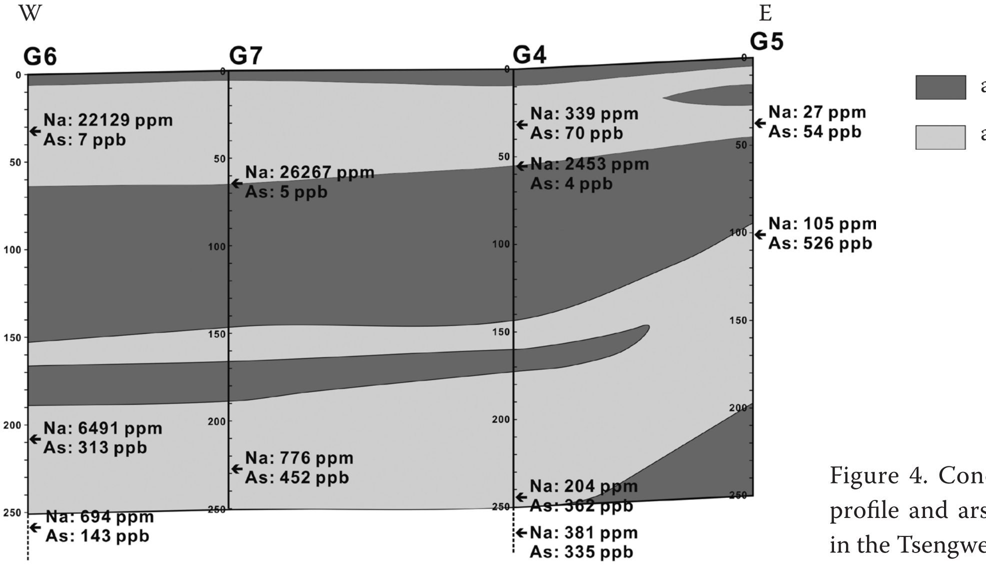

Figure 4. Conceptual hydrogeological profile and arsenic spatial distribution in the Tsengwen Creek

Table 3. Hydrochemical comparison of groundwater in shallow and deep aquifers

Aquifer	Alkalinity	Na	Mg	K	Ca	Mn	Fe
	(ppm)					(ppb)	
Shallow	278.6	12680.3	837.6	291.1	272.7	683.5	225.8
Deep	374.5	1637.9	88.7	32.0	69.0	64.5	759.8
Ratio*	1.34	0.13	0.11	0.11	0.25	0.09	3.37
P value$^+$	0.11	0.02	0.02	0.02	0.01	0.03	0.16
Aquifer	Sr	Li	V	Cr	Co	Ni	Cu
	(ppm)	(ppb)		(ppt)		(ppb)	
Shallow	6.9	4.3	2.2	24	200	1.1	152.4
Deep	1.0	6.2	3.1	200	403	2.9	14.2
Ratio*	0.15	1.45	1.44	8.52	2.02	2.66	0.09
P value$^+$	< 0.01	0.04	0.24	< 0.01	< 0.01	0.03	< 0.01
Aquifer	Zn	As	Se	Cd	Ba	Pb	U
	(ppb)			(ppt)	(ppb)	(ppt)	
Shallow	2.4	30.3	20.1	nd	950	162	13
Deep	40.4	429.4	9.8	nd	396	96	4
Ratio*	16.77	14.16	0.49	–	0.42	0.59	0.31
P value$^+$	0.14	< 0.01	0.08	–	0.27	0.33	0.03

*ratio of deep aquifer to shallow aquifer; $^+$*P* value in *t*-test

down-stream and roughly shows a negative correlation with salinity (Figure 4). Additionally, arsenic content in the shallow aquifer is much lower than that in the deep aquifer, which implies hydrogeological layering indicating two distinct hydrochemical environments. This was also evidenced by some previous studies (Lin *et al.* 2006; Selim Reza *et al.* 2012). This knowledge helps when compiling geochemical properties of sediments for describing the shallow and deep aquifers.

Table 3 lists the average values of hydrochemical properties of shallow and deep groundwater. The results show that most of the heavy metals are highly enriched in the deep aquifer including: Zn, As, Cr, Fe, Ni, and Co. Especially, the ratios comparing the deep and shallow aquifers for Zn and As, which are greater than 10. This is consistent with heavy metals being trace elements in seawater. In addition, most of elements enriched in seawater (alkaline and alkaline earth) dominate the shallow aquifer. Table 3

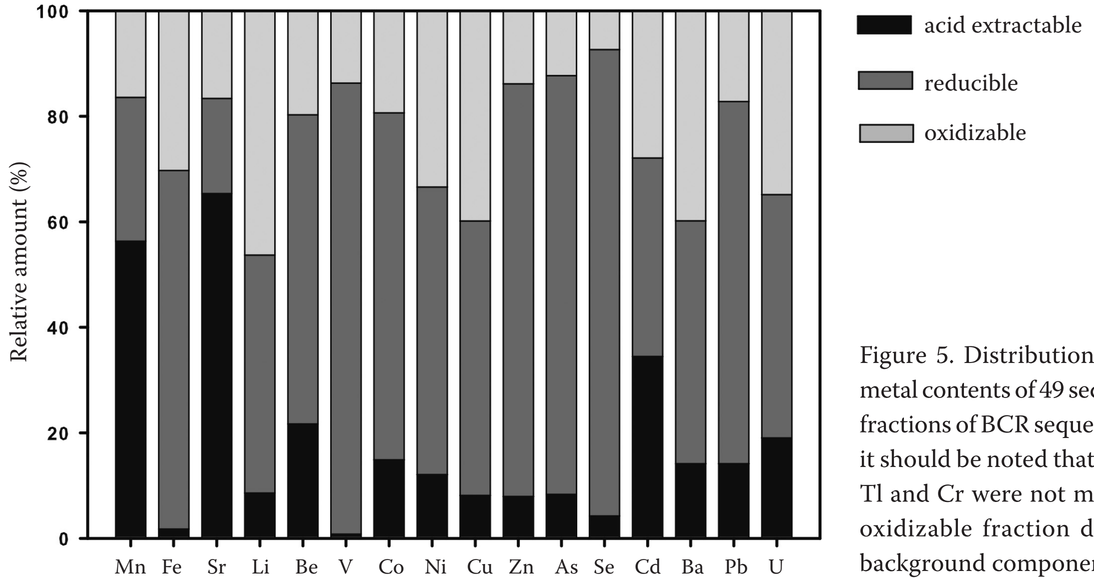

Figure 5. Distribution of the average metal contents of 49 sediments in three fractions of BCR sequential extraction; it should be noted that the contents of Tl and Cr were not measured for the oxidizable fraction due to the high background component

also gives the *P* values for independent samples *t*-tests, which demonstrate that the geochemical differences between shallow and deep water samples are significant ($P < 0.05$) for most of metals. This confirms that the two-layer hydrogeological system is appropriate for studying the geochemical property of aquifer sediments in the following.

General results of BCR. A total of 49 sediment samples were collected from 3 sites. By averaging all samples for the three phases of BCR sequential extraction, the distribution of metal contents in three fractions was obtained (Figure 5). Figure 5 demonstrates that the reducible phase is the major fraction of the total extractable heavy metals including Fe, V, Co, Ni, Cu, Zn, As, Se, and Pb. Especially notable is that over 80% of As, Zn, V, and Se are extracted from the reducible phase, which mainly bound to Fe-Mn oxides in sediments. In the acid extractable phase, only three elements, Mn, Sr, and Cd, are enriched. These elements are possibly associated with dissolution of carbonates.

By using FA, the interdependencies among measured metals in sediments are evaluated and can be subsequently used to group dependent metals into factors of geochemical meaning (Farnham *et al.* 2003; Bošnjak *et al.* 2012). The results of FA for the three extractable phases are listed in Table 4. Conclusively, three major factors can be observed in all extracted phases: (1) divalent alkaline earths, (2) transitional metals other than As and V, and

Table 4. Varimax rotated factor loading matrix of factor analysis (FA) on sediment geochemistry; significant loadings are bolded and underlined

Metal	Acid extractable				Reducible				Oxidizable			
	factor				factor				factor			
	1	2	3	4	1	2	3	4	1	2	3	4
Na	0.034	0.221	0.439	–0.223	0.599	–0.214	0.179	0.113	**0.955**	–0.165	–0.042	0.171
Mg	0.140	**0.834**	0.061	0.096	**0.772**	–0.159	0.246	–0.165	0.640	0.284	0.145	0.492
K	0.014	0.449	0.203	0.095	**0.747**	0.502	–0.028	–0.092	0.125	**0.845**	–0.180	–0.053
Ca	–0.134	**0.926**	–0.048	–0.058	0.085	–0.061	**0.978**	0.038	**0.949**	–0.158	–0.021	0.206
Mn	–0.048	**0.871**	0.139	0.078	0.385	0.346	0.611	–0.154	0.290	0.190	–0.173	**0.841**
Fe	0.227	0.065	–0.022	–0.014	**0.751**	0.373	0.075	0.379	0.443	0.393	0.178	**0.683**
Sr	–0.170	**0.933**	0.028	–0.115	0.079	0.087	**0.966**	0.104	**0.932**	–0.009	–0.002	0.224
V	**0.897**	–0.185	–0.137	–0.128	0.359	0.302	0.182	**0.838**	–0.270	–0.133	**0.826**	0.065
Cr	0.219	–0.143	**0.782**	0.183	**0.668**	0.322	–0.116	0.480	–	–	–	–
Co	**0.875**	0.034	0.315	0.114	**0.925**	–0.110	0.034	–0.047	–0.093	**0.808**	0.037	0.401
Ni	**0.934**	0.033	0.140	0.142	**0.860**	–0.043	–0.003	0.135	–0.359	**0.738**	0.158	0.270
Cu	0.345	–0.062	0.542	0.401	**0.686**	0.579	0.058	0.138	**0.867**	0.270	0.153	0.003
Zn	**0.835**	–0.005	0.205	0.200	**0.918**	0.129	0.160	0.144	0.091	**0.862**	0.030	–0.024
As	**0.704**	–0.355	–0.015	–0.145	0.033	0.023	0.001	**0.920**	0.551	0.108	**0.671**	–0.176
Se	–0.035	0.120	**0.759**	0.019	0.424	**0.715**	0.099	0.123	–	–	–	–
Cd	0.361	0.203	**0.718**	–0.359	0.226	0.097	–0.021	0.013	–0.699	–0.022	0.155	–0.115
Ba	–0.138	–0.224	–0.144	0.081	–0.080	**0.924**	–0.017	0.169	**0.927**	0.011	–0.125	0.138
Tl	–0.016	0.061	**0.899**	–0.007	–	–	–	–	–	–	–	–
Pb	–0.096	0.069	0.059	**–0.851**	0.210	0.443	0.253	–0.299	0.665	0.208	0.059	0.518
U	0.019	0.228	0.480	0.540	0.179	**0.739**	0.090	0.121	0.132	**0.795**	–0.082	0.339
Expl. Var.	4.082	3.788	3.499	1.547	6.036	3.271	2.521	2.215	6.467	3.755	1.350	2.224
Prp. Total	0.2041	0.1894	0.1750	0.0774	0.3177	0.1721	0.1327	0.1166	0.3804	0.2209	0.0794	0.1308

– not included in FA due to too many records below the detection limit

(3) As and V. The factor of divalent alkaline earths is associated with the carbonate minerals in the acid extractable phase (Factor 2). In other phases (Factor 3 in reducible phase and Factor 1 in oxidizable phase), the alkaline earth belongs to different factors and this may be caused by cation substitution and/or impurity of minerals. The metals Co, Ni, and Zn generally belong to the factor of transitional metals (Factor 1 in acid extractable and reducible phases and Factor 2 in oxidizable phase). These metals share similar ionic potential, which is defined as the ratio of electric charge to the radius. In reducible phases, this factor is obviously controlled by the dissolution of Fe-Mn oxides and more transitional metals (Fe, Cr, and Cu) are included in this factor. The factor of As and V can be found in all extractable phases. It can be explained by similar ionic potential for As and V.

Water-rock interaction. Based on the hydrogeological framework established by CA (Figure 4), the sediment samples can also be grouped into shallow and deep aquifers and the mean geochemical properties of three BCR extractable fractions are accordingly calculated as shown in Table 5 to evaluate the cumulative water-rock interaction during the long-term groundwater transportation. In the acid extractable phase, the alkaline and alkaline earth metals are highly enriched in the shallow aquifer because the area had been submerged under the seawater until 300 years ago (Figure 2d). The metals bonding with carbonate minerals (Mn, Pb, and Cd) are also enriched in the shallow aquifer due to the carbonates but As and the other transitional metals show no significant difference between the two hydrogeological units (ratio » 1 and $P > 0.05$ as demonstrated in Table 5). In the reducible and oxidizable phases, the effect of lagoon environment becomes less important and most of geochemical ratios are centralized to about 1.0 (Table 5). This means that the sediment geochemistry

Table 5. Geochemical comparison of three sediment BCR extractable phases between shallow aquifer and deep aquifer

Metal	Acid extractable			Reducible			Oxidizable		
	shallow	deep	ratio (*P*)*	shallow	deep	ratio (*P*)*	shallow	deep	ratio (*P*)*
Na (ppm)	1 741	320	0.18 (< 0.01)	27	15	0.56 (< 0.01)	525	521	0.99 (0.36)
Mg (ppm)	619	417	0.67 (0.03)	434	322	0.74 (0.05)	455	451	0.99 (0.34)
K (ppm)	191	120	0.63 (0.03)	73	58	0.80 (0.23)	86	93	1.09 (0.30)
Ca (ppm)	5 377	5 103	0.95 (0.43)	1 619	1 890	1.17 (0.17)	782	783	1.00 (0.33)
Mn (ppm)	161	116	0.72 (0.06)	73	60	0.82 (0.31)	39	40	1.03 (0.32)
Fe (ppm)	112	75	0.67 (0.06)	3 355	3 781	1.13 (0.22)	1 624	1 577	0.97 (0.46)
Sr (ppb)	19 621	16 304	0.83 (0.26)	4 606	5 158	1.12 (0.27)	4 290	4 734	1.10 (0.23)
Li (ppb)	166	215	1.29 (0.14)	1 186	866	0.73 (0.03)	949	1 110	1.17 (0.23)
V (ppb)	24	34	1.42 (0.23)	2 701	3 693	1.37 (0.05)	538	506	0.94 (0.17)
Cr (ppb)	124	118	0.96 (0.41)	1 257	1 657	1.32 (0.08)	–	–	–
Co (ppb)	539	408	0.76 (0.01)	2 378	1 817	0.76 (0.04)	550	656	1.19 (0.09)
Ni (ppb)	576	588	1.02 (0.12)	2 777	2 500	0.90 (0.24)	1 574	1 635	1.04 (0.36)
Cu (ppb)	489	437	0.89 (0.25)	2 889	2 996	1.04 (0.34)	2 048	2 429	1.19 (0.18)
Zn (ppb)	1 084	1 036	0.96 (0.09)	10 200	10 592	1.04 (0.37)	1 348	2 231	1.66 (0.02)
As (ppb)	67	93	1.39 (0.23)	542	965	1.78 (0.07)	123	117	0.96 (0.38)
Se (ppb)	29	21	0.73 (0.14)	511	525	1.03 (0.32)	–	–	–
Cd (ppb)	47	25	0.54 (< 0.01)	14	58	4.16 (0.16)	29	28	0.96 (0.32)
Ba (ppb)	2 037	3 022	1.48 (0.06)	6 757	9 673	1.43 (0.08)	6 609	7 767	1.18 (0.19)
Tl (ppb)	253	42	0.17 (0.02)	–	–	–	–	–	–
Pb (ppb)	3 008	855	0.28 (0.02)	9 867	8 209	0.83 (0.15)	2 307	2 194	0.95 (0.42)
U (ppb)	26	27	1.06 (0.31)	62	66	1.07 (0.31)	37	58	1.56 (0.12)

*ratio of deep aquifer to shallow aquifer; *P* value in *t*-test given in brackets; – not calculated due to too many records below the detection limit of the deep aquifer shows no significant difference from that of the shallow aquifer on the scale of the whole watershed. The arsenic contamination of the deep groundwater in the Tsengwen Creek watershed is not simply source-controlled and geochemical reactions along the groundwater flow path must be further evaluated. However, to compare the extractable arsenic among the three phases, the reducible phase has the most abundant amount and has the most distinct difference between two hydrogeological units (ratio = 1.78 and $P = 0.07$ in Table 5); therefore, arsenic is much possibly supplied by the dissolution of reducible phase (Fe-Mn oxides) in the deep aquifer. According to many previous studies (e.g. Anawar *et al.* 2003; McArthur *et al.* 2004), reducing geochemical environment caused by dissolution of Fe-Mn oxides is one of the most important controlling factors in the release of arsenic from sediments. In this study, all groundwater is under strong reducing condition. In addition, although arsenic is only slightly enriched in the sediments of deep aquifer, the very long residence time of groundwater may magnify the enrichment and reconfirm the derivation from geochemistry of aquifer sediments. In other words, the long residence time of groundwater could be a necessary factor for the natural arsenic contamination in the Tsengwen Creek watershed.

CONCLUSION

The results of inductively coupled plasma mass spectrometry analysis show a layered distribution of arsenic in groundwater. The deep aquifer was contaminated by high contents of arsenic. Accordingly, a conceptual hydrogeological framework with shallow and deep aquifers is established and the average sediment geochemistry of each extractable fraction for the two aquifers can be calculated on the scale of the whole watershed. The results demonstrate that arsenic and heavy metals are not significantly enriched in the deep aquifer. Therefore, the arsenic contamination of the deep groundwater in the Tsengwen Creek watershed is not simply source-controlled. On the other hand, the results of FA demonstrate that a factor with As and V can be observed in all extractable phases due to similar ionic potential. However, the reducible phase (Fe-Mn oxides) has the most abundant arsenic in the sediments and relatively significant enrichment of arsenic in the deep aquifer. With a long residence time of groundwater in the study area, the slight enrichment could be highly enhanced to achieve the observed arsenic contamination. From the above it follows that the major source of arsenic very possibly results from the dissolution of Fe-Mn oxides under a strong reducing condition, and the long residence time of groundwater could be an important and necessary factor.

Acknowledgements. This study is supported by research grants from Soil and Groundwater Pollution Remediation Fund Management Board, Environmental Protection Administration, Taiwan (EPA-99-GA103-03-A236-15).

References

Anawar H.M., Akai J., Komaki K. (2003): Geochemical occurrence of arsenic in groundwater of Bangladesh: source and mobilization processes. Journal of Geochemical Exploration, **77**: 109–131.

Anazawa K., Ohmori H. (2005): The hydrochemistry of surface waters in andesitic volcanic area, Norikura volcano, central Japan. Chemosphere, **59**: 605–615.

Baig J.A., Kazi T.G., Arain M.B., Shah A.Q., Sarfraz R.A., Afridi H.I., Kandhro G.A., Jamali M.K., Khan S. (2009): Arsenic fractionation in sediments of different origins using BCR sequential and single extraction methods. Journal of Hazardous Materials, **167**: 745–751.

Bošnjak M.U., Capak K., Jazbec A., Casiot C., Sipos L., Poljak V., Dadić Ž. (2012): Hydrochemical characterization of arsenic contaminated alluvial aquifers in Eastern Croatia using multivariate statistical techniques and arsenic risk assessment. Science of the Total Environment, **420**: 100–110.

Farnham I.M., Johannesson K.H. Singh A.K. Hodge V.F., Stetzenbach K.J. (2003): Factor analytical approaches for evaluating groundwater trace element chemistry data. Analytica Chimica Acta, **490**: 123–138.

Guggenmos M.R., Daughney C.J., Jackson B.M., Morgenstern U. (2011): Regional-scale identification of groundwater-surface water interaction using hydrochemistry and multivariate statistical methods, Wairarapa Valley, New Zealand. Hydrology and Earth System Sciences, **15**: 3383–3398.

Hsieh M.L., Knuepfer P.L.K. (2001): Middle-late Holocene river terraces in the Erhjen River Basin, southwestern Taiwan: implications of river response to climate change and active tectonic uplift. Geomorphology, **38**: 337–372.

Irawan D.E., Puradimaja D.J., Notosiswoyo S., Soemintadiredja P. (2009): Hydrogeochemistry of volcanic hydrogeology based on cluster analysis of Mount Ciremai, West Java, Indonesia. Journal of Hydrology, **376**: 221–234.

Li Z.H., Hong H.L., Jean J.S., Koski A.J., Liu C.C., Selim Reza A.H.M, Randolph J.J., Kurdas S.R., Friend J.H., Antinucci S.J. (2011): Characterization on arsenic sorption and mobility of the sediments of Chia-Nan Plain, where Blackfoot disease occurred. Environmental Earth Sciences, **64**: 823–831.

Lin Y.B., Lin Y.P., Liu C.W., Tan Y.C. (2006): Mapping of spatial multi-scale sources of arsenic variation in groundwater on ChiaNan floodplain of Taiwan. Science of the Total Environment, **370**: 168–181.

Liu C.W., Lin K.H., Kuo Y.M. (2003): Application of factor analysis in the assessment of groundwater quality in a blackfoot disease area in Taiwan. Science of the Total Environment, **313**: 77–89.

Lu F.J. (1990): Blackfoot disease: arsenic or humic acid? The Lancet, **336**: 115-116.

Lu H.Y., Liu T.K., Chen W.F., Peng T.R., Wang C.H., Tsai M.H., Liou T.S. (2008): Use of geochemical modeling to evaluate the hydraulic connection of aquifers: A case study from Chianan Plain, Taiwan. Hydrogeology Journal, **16**: 139-154.

McArthur J.M., Banerjee D.M., Hudson-Edwards K.A. (2004): Natural organic matter in sedimentary basins and its relation to arsenic in anoxic ground water: the example of West Bengal and its worldwide implications. Applied Geochemistry, **19**: 1255–1293.

Rauret G., Lopez-Sanchez J.F., Sahuquillo A., Rubio R., Davidson C., Ure A., Quevauviller P. (1999): Improvement of the BCR three step sequential extraction procedure prior to the certification of new sediment and soil reference materials. Journal of Environmental Monitoring, **1**: 57–61.

Selim Reza A.H.M., Jean J.S., Lee M.K., Kulp T.R., Hsu H.F., Liu C.C., Lee Y.C. (2012): The binding nature of humic substances with arsenic in alluvial aquifers of Chianan Plain, southwestern Taiwan. Journal of Geochemical Exploration, **114**: 98–108.

Tseng W.P., Chen W.Y., Sung J.L., Chen J.S. (1961): A clinical study of Blackfoot Disease in Taiwan, an endemic peripheral vascular disease. Memoire College Medicinal, National Taiwan University **7**: 1–18.

Ure A., Quevauviller P.H., Muntau H., Griepink B. (1992): EUR report. CEC Brussels, **14763**: 1992:85.

Wang S.W., Liu C.W., Jang C.S. (2007): Factors responsible for high arsenic concentration in the groundwater catchments in Taiwan. Applied Geochemistry, **22**: 460–476.

Whalley C., Grant A. (1994): Assessment of the phase selectivity of the European Community bureau of reference (BCR) sequential extraction procedure for metals in sediment. Analytica Chimica Acta, **291**: 287–295.

Received for publication July 4, 2013
Accepted after corrections November 14, 2013

Corresponding author:

Assoc. Prof Hsueh-Yu Lu, National Chung Cheng University, Department of Earth and Environmental Sciences,
168 University Rd., Min-Hsiung Chia-Yi, Taiwan; e-mail: sheilu@ccu.edu.tw